Experimental study of shape coexistence in ^{189}Tl

S. K. Chamoli, Rajesh Kumar, and I. M. Govil

Department of Physics, Panjab University, Chandigarh 160014, India

P. Joshi

Department of Physics, Panjab University, Chandigarh 160014, India and
Nuclear Science Centre, Post Box No. 10502, New Delhi 110067, India

R. P. Singh, S. Muralithar, and R. K. Bhowmik

Nuclear Science Centre, Post Box No. 10502, New Delhi 110067, India

The shape coexistence phenomena in ^{189}Tl are investigated by measuring the lifetimes of the high spin states through the recoil distance LIFETIME measurement technique. For this study, the ^{165}Ho(^{28}Si, $4n$)^{189}Tl reaction at a beam energy of 138 MeV was used. In this measurement, the lifetimes of four levels of the negative parity $\pi h_{9/2}$ band and seven levels of the positive parity $\pi i_{13/2}$ band are found. The extracted transition quadrupole moments for the positive parity $\pi i_{13/2}$ band show interesting changes with increasing level spin. This band starts with a small oblate shape ($Q_t = 1.1$ e b) at low spin ($17/2^+$) and attains a strongly deformed prolate shape ($Q_t = 8.8$ e b) at high spins ($33/2^+$). On the other hand, the negative parity $\pi h_{9/2}$ band shows a stable oblate structure against the increasing spin with an average quadrupole moment (Q_t) of $\sim$2.6 e b. To better understand the shape coexistence phenomena in ^{189}Tl nucleus, the experimental results are also compared with the results of the total Routhian surfaces calculations, for the positive parity $\pi i_{13/2}$ and the negative parity $\pi h_{9/2}$ bands in this nucleus. The comparison confirms the shape coexistence structure of the ^{189}Tl nucleus in the positive parity $\pi i_{13/2}$ configuration.

I. INTRODUCTION

The Tl nuclei with mass $A \sim 190$ are well known for the prolate-oblate shape coexistence in their structure. A number of spectroscopic studies [1–6] have shown that these nuclei have an oblate ground state built on the negative parity $\pi h_{9/2}$ ($K = 9/2^-$) band and the positive parity $\pi i_{13/2}$ ($K = 13/2^+$) band, while at high excitations they are found to acquire a well-deformed prolate structure ($\beta_2 \sim 0.2$–0.3) and, in some cases [7–16], even a super-deformed structure ($\beta_2 \sim 0.5$–0.6) at still higher excitations. The types of orbitals responsible for giving these prolate deformed shapes in Tl nuclei at high excitations, however, are inconsistent. In case of ^{185,187}Tl nuclei, the low-$K \pi i_{13/2}[660]1/2^+$ and the $\pi h_{9/2}[532]3/2^-$ orbitals coupled to the prolate Hg core give prolate shapes to these nuclei at high excitation. On the other hand, for the heavier Tl nuclei ($A \geqslant 189$), only one band associated with the $\pi i_{13/2}[660]1/2^+$ orbital is observed to give the prolate deformed shapes at high spins.

Several physical processes have been suggested to justify this inconsistency of prolate structure in Tl nuclei at high spins, but the one suggested by Porquet *et al.* [2] on the basis of the Pauli blocking effect and the one by Lane *et al.* [5] based on the deformation effect seem to be the most realistic. According to Porquet *et al.* [2], the absence of prolate $\pi h_{9/2}$ structure in heavier Tl nuclei ($A \geqslant 189$) is due to the pushing up of this orbital in energy as a result of the significant loss in pairing correlation of the core caused by the Pauli blocking of the $\pi h_{9/2}$ orbital in the presence of the prolate Hg core of $(\pi h_{9/2})^2$ configuration. Lane *et al.* [5], on the other hand,

predict this absence of prolate $\pi h_{9/2}$ structure in heavier Tl nuclei as due to the decrease in the deformation of this band in moving away from the neutron midshell ($N = 104$).

Thus, in order to check the deformation aspect of the observed inconsistency in the prolate structure in Tl nuclei at high spins and to verify the prolate-oblate shape coexistence, it is important to perform shape studies in Tl nuclei with $A \geqslant 185$. For such studies, the quadrupole moment, which is a direct signature of the intrinsic deformation and hence the shape of the nucleus, is required to be measured with high precision. However, no such measurements have been carried out in the past for the positive parity $\pi i_{13/2}$ and the negative parity $\pi h_{9/2}$ ground state bands in any of these most-neutron-deficient Tl nuclei with $A \geqslant 185$. Using the rotational model [17], the quadrupole moment can be easily extracted from the measured nuclear level LIFETIME.

So, with this motivation, for the first time we performed LIFETIME measurements for different quasiproton bands in the ^{187,189}Tl nuclei ($N = 106, 108$, respectively) with the recoil distance Doppler shift method (RDM). The results of the LIFETIME measurement study on the ^{187}Tl nucleus [18] confirmed the prolate-oblate shape coexistence for this nucleus in both the negative parity $\pi h_{9/2}$ and the positive parity $\pi i_{13/2}$ configurations. The studies also confirmed that the average deformation of the $h_{9/2}$ band is somewhat less than the $i_{13/2}$ band in ^{187}Tl nucleus.

The present study of LIFETIME measurement in ^{189}Tl is essentially required to verify Lee's prediction of the decrease in the deformation of the $\pi h_{9/2}$ band in moving away from the

neutron midshell of $N = 104$, i.e., from ^{187}Tl ($N = 106$) to ^{189}Tl ($N = 108$). During the past decade, most of the studies on this nucleus were focused on the issue of the existence and properties of the super deformation at high excitation [7–16]. Doppler shift attenuation LIFETIME measurements (DSAM) were also carried out by W. Reviol [11] to find the deformation of the high spin super-deformed band in ^{189}Tl, but the issue of deformation measurements in the ground state bands in ^{189}Tl remained untouched.

The present work is the first attempt to measure the deformation of the positive parity $\pi i_{13/2}$ and the negative parity $\pi h_{9/2}$ ground state bands in ^{189}Tl. To fully understand and interpret the experimental results, the total Routhian surfaces (TRS) calculations within the cranked Hartree-Fock-Bogoliubov model [19–23] are also done for both the negative parity $\pi h_{9/2}$ and the positive parity $\pi i_{13/2}$ configurations in ^{189}Tl nucleus, which suggest an oblate configuration for the $h_{9/2}$ band and a prolate configuration for the $i_{13/2}$ band at higher excitation. The prolate-oblate assignments to the bands in both the negative parity $\pi h_{9/2}$ and the positive parity $\pi i_{13/2}$ configurations, used in the present manuscript, are based on the γ-ray spectroscopy work of Porquet *et al.* [2] and W. Reviol *et al.* [6] on ^{189}Tl.

II. EXPERIMENTAL DETAILS

In the present study, the ^{189}Tl nucleus was populated in the ^{165}Ho(^{28}Si, $4n$)^{189}Tl reaction at a beam energy of 138 MeV at the Nuclear Science Center (NSC), New Delhi. This energy provided a velocity of $\beta(=v/c) \sim 1\%$ to the recoiling ^{189}Tl ions in the present experiment. The well-focused beam of ^{28}Si, accelerated by the 15 UD Pelletron, was allowed to fall on a $\sim$1 mg/cm^2 thick self-supporting target foil of ^{165}Ho. A self-supporting gold foil of thickness $\sim$10 mg/cm^2 was used to stop the recoils produced in the reaction. Both the target and the stopper foils were properly mounted and well stretched on two identical metal cones at the two ends of the NSC plunger device with target foil facing the beam. The distance calibration was done by the capacitance method [24], and the minimum distance between the target and stopper foils (d_0) was found to be $\sim$14 μm. The data were collected for different target-stopper distances ranging from 14 to 10000 μm in 24 unequal steps. The γ rays were detected with the γ detector array (GDA) setup at NSC, consisting of 12 Compton-suppressed high-purity Ge detectors arranged in three different rings having four detectors each and making an angle of 50°, 99°, and 144° with the beam direction. A 14-element bismuth germanate (BGO) multiplicity filter array was also used. The data were collected in the singles mode with the BGO multiplicity condition $M \geqslant 2$. This BGO gating condition helped in cleaning the energy spectra significantly by reducing the background coming from low multiplicity processes such as Coulomb excitation, radioactivity, etc. We confirmed the level scheme for ^{189}Tl nucleus in our experiment as reported earlier by Porquet *et al.* [2], and it is shown in Fig. 1.

III. DATA ANALYSIS

During the online analysis with few data files, our observation of the individual Ge detector spectra found that the
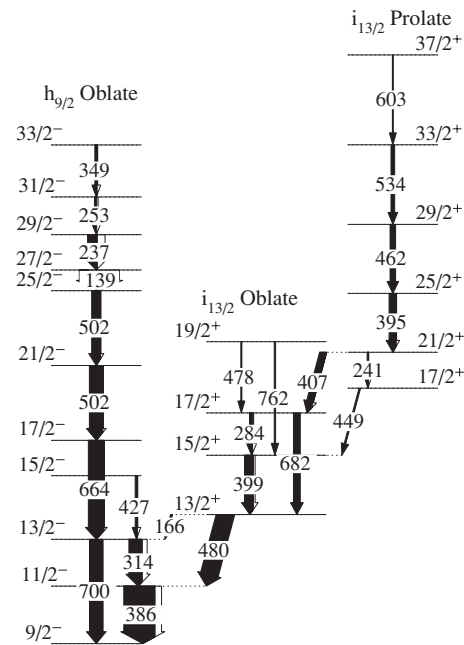

FIG. 1. Partial level scheme of ^{189}Tl, relevant to this work showing different quasiproton bands for which LIFETIME measurement is done. Widths of transitions are proportional to γ-ray intensities. Full level scheme appears in Ref. [2].

detectors at the forward angle of 50° had much better resolution and hence better separation of the shifted and the unshifted peaks than did the detectors at the backward angle of 144°. However, we checked that the shift of the corresponding peaks was in the right direction at the backward angle. We therefore decided to concentrate only on the forward angle detectors and collected the data for detectors at 50° and 99° with respect to the beam direction. The singles data of all four detectors at one angle, after proper gain matching in the software, were added together, and two raw spectra corresponding to the detectors at 50° and 99° were produced. Since in the present experiment the recoil velocity obtained is $\sim$1% of the speed of light, hardly any shift in the γ energies was observed in the summed spectra of the four detectors at 99°. Hence, this spectrum was used to check the actual centroid of the unshifted γ-energy peaks and the possibility of any contamination in the γ-energy peaks of interest. However, no significant contamination was found in any of the γ energy considered.

A portion of raw spectrum showing the shifted (S) and unshifted (U) peaks of a few γ transitions of interest in ^{189}Tl at four different target-stopper distances at an angle of 50° with respect to the beam direction is shown in Fig. 2. In the analysis, the forward angle detectors' spectra at each target-stopper distance were fitted to obtain the areas of the shifted and unshifted peaks, which after applying the efficiency correction, resulted in the intensity of the unshifted (U) and the shifted (S) γ-ray energy. The normalization of intensities is basically done with the Coulomb excited gold peak at 547 keV, observed in the spectrum. However, as a double check, the intensity of the unshifted γ ray (U) is also normalized to the total intensity ($S + U$) at all distances for each γ transition of interest. The resulting normalized intensity
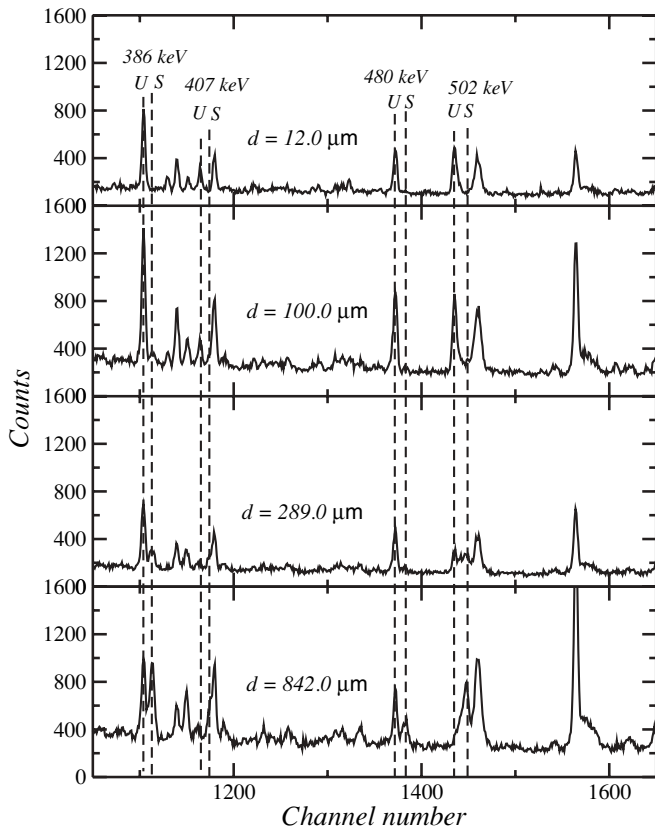
FIG. 2. Portions of raw spectra showing shifted (S) and unshifted (U) peaks of a few γ transitions of interest in ^{189}Tl at four different target-stopper distances ($d_{\text{T}-\text{S}}$) at an angle of $50°$ with respect to the beam direction.

of the unshifted γ transitions are then analyzed with the computer program LIFETIME [25]. This program allows the simultaneous description of the time dependence of moving and stopped components for each γ transition and finds the level LIFETIME by making a least-squares fit to their intensities with initial level populations, and transition probabilities are treated as variable parameters.

The errors in the measured lifetimes are found by using a subroutine MINUIT [26] included in the LIFETIME program. The errors include statistical errors, fitting errors, and errors arising from correlation between the parameters. The correlated errors from the fitting process are estimated by examining the behavior of chi-square ($\chi^2_{\min}$) in the vicinity of the best value of the parameter.

In the data analysis, two types of feeding are considered at each level, namely, the cascade feeding from the above and the side feeding, except for the highest level, for which only the feeding from the top is assumed through an unknown rotational band of constant quadrupole moment. The quadrupole moment of this modeled rotational band and the initial population of the highest level are treated as variable parameters. The other finer details of the data analysis are given elsewhere [18].

In the case of the negative parity $\pi h_{9/2}$ band, the two successive γ transitions, $25/2^- \rightarrow 21/2^-$ and $21/2^- \rightarrow 17/2^-$, are multiplet with both having the same 502 keV energy

(Fig. 1). So during the data analysis of this band, special care is taken to extract the level lifetimes of the two levels having spins of $25/2^-$ and $21/2^-$ involved in this multiplet. Porquet *et al.* [2] in their γ-ray spectroscopy work have shown that the intensity of the two 502 keV $E2$ transitions from $25/2^- \rightarrow 21/2^-$ and $21/2^- \rightarrow 17/2^-$ are in the ratio of 2:3. So, at first the normalized unshifted (U) and the shifted (S) energy peak intensities of the 502 keV γ transition were measured at every target-stopper distance. Now, since the level lifetimes depend strongly on the γ transition energies ($\tau \propto 1/E_\gamma^5$) and keeping in mind that the two levels are consecutive high spin levels of the same rotational band decaying by the same energy (502 keV) γ transitions, these are not expected to have very different lifetimes. Therefore, the normalized intensity of the unshifted 502 keV γ-energy peak is divided in the ratio of 2:3 suggested by Porquet *et al.* [2] to get the unshifted intensities of the $25/2^- \rightarrow 21/2^-$ and $21/2^- \rightarrow 17/2^-$ (502 keV) γ transitions, respectively. The normalized unshifted intensities so obtained were then used for the LIFETIME analysis considering the $25/2^- \rightarrow 21/2^-$ and $21/2^- \rightarrow 17/2^-$ as two independent transitions in the LIFETIME program.

In the present analysis for both the $\pi h_{9/2}$ and $\pi i_{13/2}$ bands, the side feeding levels do not seem to have much influence on the level lifetimes. For every γ transition considered in the present analysis, the major part of the intensity comes through the cascade feeding from the level above it, and a very small portion comes from the side feeding level. Furthermore, the fitted values of the side feeding level lifetimes are found to be much smaller than the respective level fed by them for all the transitions in both the bands.

IV. RESULTS AND DISCUSSION

The intensity decay curves of the normalized unshifted γ rays as a function of the target-stopper distance for the observed γ transitions for the negative parity $\pi h_{9/2}$ and positive parity $\pi i_{13/2}$ bands are shown in Figs. 3 and 4, respectively, and the results of the LIFETIME measurements for these bands are tabulated in Tables I and II, respectively. These results are obtained for detectors positioned at the forward angle of $50°$ with respect to the beam direction in the laboratory frame.

From the measured level lifetimes, the reduced transition probability $B(E2)$ and the reduced transition quadrupole moments Q_t are extracted using the rotational model [17]. To see the effect of rotation on the deformation properties, the transition quadrupole moments Q_t for the $\pi h_{9/2}$ and $\pi i_{13/2}$ bands are plotted as a function of spin in Fig. 5. In Table I, the low values of transition quadrupole moments for the $\pi h_{9/2}$ band strongly indicate that this band has a very small deformation. The average value of the transition quadrupole moment for this highly coupled oblate band is $2.6(0.8)$ e b, which on assuming the axial symmetry of the nucleus, corresponds to $\beta_2 = 0.09(2)$. The nearly constant nature of the measured $B(E2)$ values with spin indicates that this band does not undergo any serious interaction with other neighboring bands, thus preserving its properties.
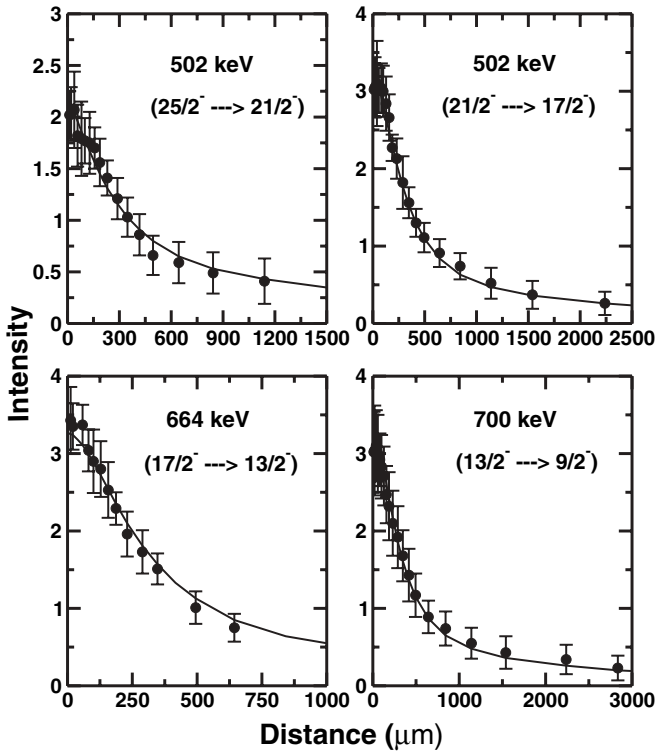
FIG. 3. Intensity decay curves for unshifted γ-ray transitions of negative parity $\pi h_{9/2}$ band in ^{189}Tl.

FIG. 4. Intensity decay curves for unshifted γ-ray transitions of the positive parity $\pi i_{13/2}$ band in ^{189}Tl.

However, on looking at the level lifetimes for this band in Table I, a very interesting behavior in their values as a function of spin is seen. The upper levels in the band, i.e., the $25/2^-$ and $21/2^-$ levels, are found to have larger lifetimes (extracted with model-dependent assumptions) than the lifetimes of the lower levels in the decay cascade, i.e., the $17/2^-$ and $13/2^-$ levels. From Fig. 1, it is clear that this band is not a regular collective band; but on the contrary, it has a single-particle nature with a few collective transitions. For the collective transitions, the γ-ray energy is found to be decreasing with increase in spin along the band, which is contrary to the trend found in the normal collective bands, where the γ-ray energy goes on increasing with increasing spin [$E_{\rm rot} \propto I(I + 1)$]. Because the level LIFETIME depends strongly on the γ transition energies ($\tau \propto 1/E_{\gamma}^5$), the increase in the level lifetimes with spin as observed for this band does not effect the $B(E2)$ values.

On the other hand, for the positive parity $\pi i_{13/2}$ band, which looks like a normal rotational band at high spins (Fig. 1), the
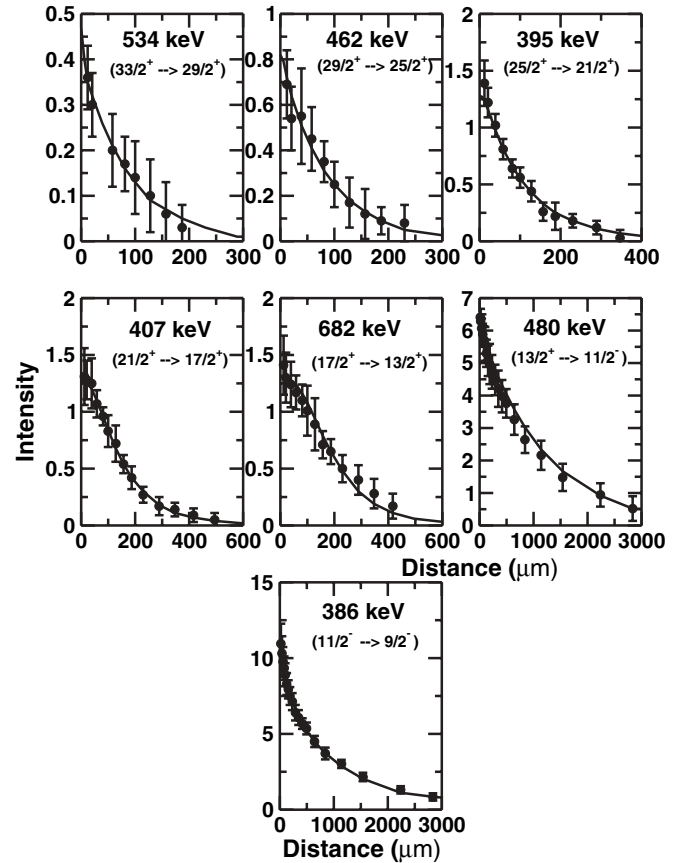
transition quadrupole moment shows an intriguing behavior with spin. At low spin ($17/2^+$), this band has a very low value of quadrupole deformation ($\beta_2 = 0.04$); but with an increase in spin, a very large increase in the value of β_2 is observed. This large change in the value of β_2 between $17/2^+$ (0.04) and $21/2^+$ (0.13) is an indication of the major structural changes taking place in this configuration between these two spins. A similar change in deformation at the same spin in the positive parity band is also seen in ^{187}Tl [18]. As is clear from the partial level scheme shown in Fig. 1, the $17/2^+$ to $21/2^+$ transition ($E_\gamma = 407$ keV) is the linking transition between the oblate and prolate rotational sequences of the positive parity $\pi i_{13/2}$ band, so the sharp increase in the quadrupole moment indicates a very little mixing of the oblate ground

TABLE I. Experimental results for different γ transitions in proton quasiparticle $\pi h_{9/2}$ band in ^{189}Tl.

S.No.	Energy (keV)	Transition $(I_i^\pi \rightarrow I_f^\pi)$	LIFETIME (ps)	$B(E2)$ $(e^2\,{\rm b}^2)$	Q_t $(e\,{\rm b})$	β_2
1	700.0	$\frac{13}{2}^- \rightarrow \frac{9}{2}^-$	2.7 ± 0.8	0.17 ± 0.04	2.3 ± 0.3	0.08 ± 0.01
2	664.0	$\frac{17}{2}^- \rightarrow \frac{13}{2}^-$	2.6 ± 0.6	0.24 ± 0.05	2.7 ± 0.3	0.09 ± 0.01
3	502.0	$\frac{21}{2}^- \rightarrow \frac{17}{2}^-$	10.3 ± 2.1	0.23 ± 0.05	2.5 ± 0.3	0.08 ± 0.01
4	502.0	$\frac{25}{2}^- \rightarrow \frac{21}{2}^-$	<8.8	>0.27	>2.8	>0.1

TABLE II. Experimental results for different γ transitions in proton quasiparticle $\pi i_{13/2}$ band in ^{189}Tl.

S.No.	Energy (keV)	Transition $(I_i^\pi \to I_f^\pi)$	LIFETIME (ps)	$B(E2)$ $(e^2\,b^2)$	Q_t $(e\,b)$	β_2
1	386.0	$\frac{11}{2}^- \to \frac{9}{2}^-$	54.5 ± 5.0	–	–	–
2	480.0	$\frac{13}{2}^+ \to \frac{11}{2}^-$	301.0 ± 16.6	–	–	–
3	682.0	$\frac{17}{2}^+ \to \frac{13}{2}^+$	13.0 ± 1.6	0.04 ± 0.01	1.1 ± 0.1	0.04 ± 0.01
4	407.0	$\frac{21}{2}^+ \to \frac{17}{2}^+$	12.4 ± 1.7	0.48 ± 0.07	3.8 ± 0.3	0.13 ± 0.01
5	395.0	$\frac{25}{2}^+ \to \frac{21}{2}^+$	3.0 ± 0.4	2.12 ± 0.28	7.8 ± 0.5	0.27 ± 0.02
6	462.0	$\frac{29}{2}^+ \to \frac{25}{2}^+$	1.3 ± 0.2	2.55 ± 0.44	8.6 ± 0.8	0.30 ± 0.03
7	534.0	$\frac{33}{2}^+ \to \frac{29}{2}^+$	<1.0	>2.70	>8.8	>0.31

state band with a coexisting excited prolate band during the change in the odd particle's orbit from oblate to prolate. Again, a further increase of nearly 100% in the value of the transition quadrupole moment between spins $21/2^+$ and $25/2^+$ indicates that the nucleus undergoes a major centrifugal stretching in the prolate excited band, which is a consequence of the softness of the nucleus. This fact is qualitatively supported by the self-consistent total energy calculations done for different bands in ^{189}Tl by Reviol *et al.* [6].

The continuous increase in the deformation even after $25/2^+$ spin is an indication of a highly deformed prolate structure of the ^{189}Tl nucleus in this configuration. The average value of $Q_t = 8.4(1.0)$ e b for this prolate band, which corresponds to $\beta_2 \sim 0.29$, is found to be higher than that in ^{187}Tl and in the other normally deformed ($\sim$0.25) prolate nuclei of this mass region [27–32]. In these nuclei, the higher deformation of this positive parity $\pi i_{13/2}[660]1/2^+$ band is interpreted as being caused by the highly deformation-driving nature of this intruder configuration. The same interpretation can be given here also, because around $Z = 82$, this configuration is found
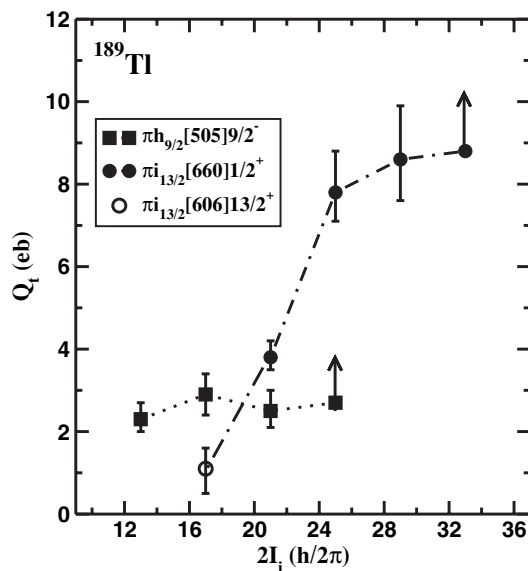
to be the lowest in energy at $\beta_2 \sim 0.3$ and therefore available to be occupied by the odd particle in Tl nuclei. Additionally, in almost all the Tl nuclei in which the super deformation is observed [7–16], this low-K, $\pi i_{13/2}$ configuration is found to be responsible for giving such highly deformed structures. So the observed high deformation in ^{189}Tl is mainly a result of the enhanced stretching of the soft even-even nuclear core by the $\pi i_{13/2}$ orbital.

The softness of the nuclear potential in ^{189}Tl is also being noticed in the TRS calculations. The results of these calculations for both the negative parity, positive signature $(\pi h_{9/2})$, and the positive parity, positive signature $(\pi i_{13/2})$ bands in ^{189}Tl at different rotational frequencies are shown in Fig. 6. From the plots, it is observed that in both the bands, the ^{189}Tl nucleus shows oblate deformation in the ground state
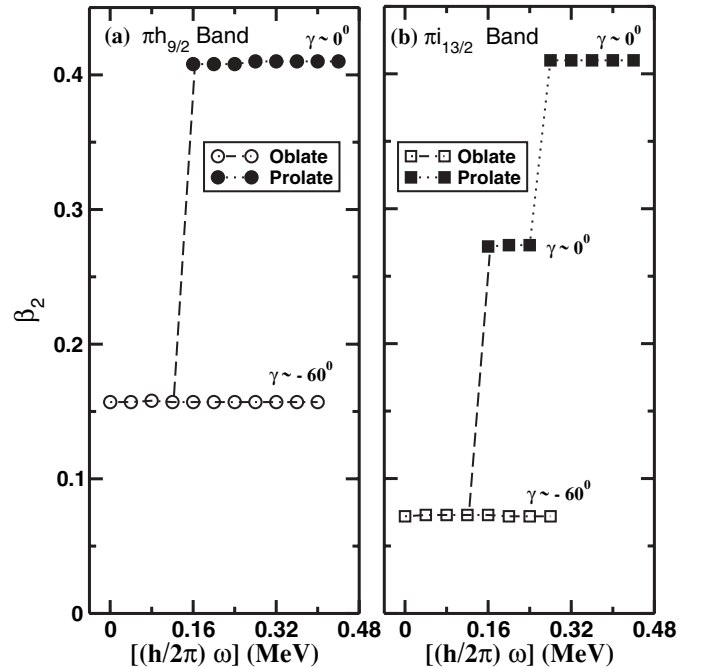
FIG. 5. Plot of variation of observed transition quadrupole moment Q_t with spin I for both the $\pi h_{9/2}$ and $\pi i_{13/2}$ bands in ^{189}Tl. On the x axis, spin values are written after multiplying by 2.

FIG. 6. Plot of TRS calculated β_2 and γ deformation parameters as a function of rotational frequency for negative parity, positive signature $\pi h_{9/2}$ band and positive parity, positive signature $\pi i_{13/2}$ band in ^{189}Tl.

($\hbar\omega = 0.0$) but indicates a rapid change of shape from oblate to highly deformed prolate at high excitation and spin. This rapid change of nuclear shape reflects the highly soft nature of nuclear potential for the ^{189}Tl nucleus corresponding to these two configurations. In the positive parity $\pi i_{13/2}$ configuration, this softness of nuclear potential leads to high deformations and even to the super deformations in this nucleus. The observation of high deformation for this positive parity prolate $\pi i_{13/2}$ band in the present study is a clear manifestation of the effect of highly deformation-driving orbitals on the soft even-even nuclear core.

On the other hand, for the negative parity $\pi h_{9/2}$ band, the TRS calculations show the change of structure from normally deformed oblate to strongly deformed prolate for $\hbar\omega \geqslant 0.16$ MeV (Fig. 6). However, the experimental lifetimes do not indicate any such impression nor is it manifested at higher excitation in the energy level diagram as reported by Porquet *et al.* (Fig. 1). Experimentally, this band is found to have a very stable oblate structure ($\beta_2 \sim 0.09$) which does not undergo any significant deformation changes. The presence of the prolate $\pi h_{9/2}$ structure in ^{187}Tl (106) [18] and its absence in the ^{189}Tl ($N = 108$) thus supports the prediction of a decrease in the deformation of this band in moving away from the neutron midshell of $N = 104$ in Tl nuclei as reported by Lane *et al.* [5].

V. SUMMARY

In the present work, the prolate-oblate shape coexistence in ^{189}Tl is investigated experimentally by the LIFETIME measurement technique. For this purpose, the nuclear level lifetimes of the high spin states of both the negative parity $\pi h_{9/2}$ and the positive parity $\pi i_{13/2}$ bands were measured with the RDM method. For the positive parity $\pi i_{13/2}$ band, the extracted deformation parameter β_2 shows very intriguing

behavior with spin. At low spins ($17/2^+$), this band has a very small oblate deformation ($\beta_2 = 0.04$) in the ground state; it has a prolate-oblate structure at midfrequencies; and at high spins, it acquires a very strong prolate deformation ($\beta_2 \sim 0.29$). This is the first observation of a prolate structure with β_2 lying between the normally deformed (0.23) and the super-deformed (0.45) structures observed in Tl nuclei.

The high deformation of the $\pi i_{13/2}[660]1/2^+$ band is interpreted as a consequence of the deformation-driving property of this low-K band on the highly soft even-even nuclear core. The observation of the oblate shape at low frequencies, oblate-prolate shapes at midfrequencies, and pure prolate shape at high frequencies in the prolate $i_{13/2}$ band is a clear manifestation of the shape coexistence structure of ^{187}Tl for this configuration.

For the negative parity $\pi h_{9/2}$ band, on the other hand, no significant changes in the value of deformation with spin are observed, with β_2 remaining almost constant at ~ 0.09. The lack of drastic changes in deformation with spin along this band shows the stability of the oblate structure. The absence of a prolate $\pi h_{9/2}$ structure in ^{189}Tl (108) and its presence in ^{187}Tl (106) thus support the prediction of Lane *et al.* regarding the decrease in the deformation of this band in moving away from the neutron midshell ($N = 104$) in Tl nuclei.

[1] A. J. Kreiner *et al.*, Phys. Rev. C **38**, 2674 (1988).
[2] M. G. Porquet *et al.*, Phys. Rev. C **44**, 2445 (1991).
[3] W. Reviol *et al.*, Phys. Rev. C **49**, R587 (1994).
[4] G. J. Lane *et al.*, Phys. Lett. **B324**, 14 (1994).
[5] G. J. Lane *et al.*, Nucl. Phys. **A586**, 316 (1995).
[6] W. Reviol *et al.*, Phys. Scr. **T56**, 167 (1995).
[7] W. Reviol *et al.*, Phys. Rev. C **58**, R2644 (1998).
[8] M. P. Carpenter *et al.*, Nucl. Phys. **A557**, 57c (1993).
[9] S. Pilotte *et al.*, Phys. Rev. C **49**, 718 (1994).
[10] W. Reviol *et al.*, Nucl. Phys. **A630**, 434c (1998).
[11] W. Reviol, J. Res. Natl. Inst. Stand. Technol. **105**, 153 (2000).
[12] F. Azaiez *et al.*, Z. Phys. A **336**, 243 (1990); Nucl. Phys. **A520**, 121c (1990) .
[13] F. Azaiez *et al.*, Phys. Rev. Lett. **66**, 1030 (1991).
[14] R. Krucken *et al.*, Eur. Phys. J. A **5**, 367 (1999).
[15] S. Bouneau *et al.*, Eur. Phys. J. A **2**, 245 (1998).
[16] F. Azaiez *et al.*, Phys. Scr. T **56**, 35 (1995).
[17] S. G. Nilsson and I. Ragnarsson, *Shapes and Shells in Nuclear Structure* (Cambridge University Press, Cambridge, England, 1995), p. 290.
[18] S. K. Chamoli *et al.*, Phys. Rev. C **71**, 054324 (2005).

[19] P. Ring and P. Schuck, *The Nuclear Many Body Problems* (Springer-Verlag, Berlin, 1980), p. 244.
[20] W. Nazarewicz, M. A. Riely, and J. D. Garrett, Nucl. Phys. **A512**, 61 (1990).
[21] T. R. Werner and J. Dudek, At. Data Nucl. Data Tables **59**, 1 (1995).
[22] T. R. Werner and J. Dudek, At. Data Nucl. Data Tables **50**, 179 (1992).
[23] V. M. Strutinsky, Yad. Fiz. **3**, 614 (1966); Nucl. Phys. **A95**, 420 (1967).
[24] T. K. Alexander and A. Bell, Nucl. Instrum. Methods **81**, 22 (1970).
[25] J. C. Wells *et al.*, Report No. ORNL/TM-9105 (1985).
[26] F. James and M. Roose, Comput. Phys. Commun. **10**, 343 (1975).
[27] S. K. Chamoli *et al.*, Phys. Rev. C **66**, 024307 (2002).
[28] P. Joshi *et al.*, Phys. Rev. C **60**, 034311 (1999).
[29] P. Joshi *et al.*, Phys. Rev. C **64**, 034303 (2001).
[30] D. Muller *et al.*, Phys. Lett. **B332**, 265 (1994).
[31] P. Joshi *et al.*, Phys. Rev. C **66**, 044306 (2002).
[32] P. Joshi *et al.*, Phys. Rev. C **69**, 044304 (2004).